FINAL REPORT

# STUDIES OF ATMOSPHERIC REFRACTION EFFECTS ON LASER DATA

(NASA-CR-170503) STUDIES OF ATMOSPHERIC REFRACTION EFFECTS ON LASER DATA Final Report (EG & G Washington Analytical Services) 57 p HC A04/MF A01 CSCL 20E N83-22583
G3/36 Unclas 09816

Peter J. Dunn and William A. Pearce
EG&G Washington Analytical Services Center, Inc.
6801 Kenilworth Avenue
Riverdale, Maryland 20737

Thomas S. Johnson
Instrument Electro-Optics Branch
Goddard Space Flight Center
Greenbelt, Maryland 20771

Contract No. NAS 5-25884

June 1982

TABLE OF CONTENTS


| | |
|---|---|
| INTRODUCTION | 1 |
| REFRACTIVITY AT OPTICAL FREQUENCIES | 4 |
| The Dry Term | 4 |
| The Wet Term | 7 |
| REFRACTION CORRECTION OF SATELLITE MEASUREMENTS | 9 |
| Variations in the Real Atmosphere | 11 |
| Analysis of Radiosonde Observations in New Mexico | 13 |
| Three Dimensional Ray-Tracing Procedure | 14 |
| Numerical Methods | 16 |
| Assessment of the Vertical Profile Observations | 17 |
| The Effect of Temperature Gradients on Refractivity | 19 |
| INTEGRITY OF METEOROLOGICAL OBSERVATIONS | 21 |
| GEODETIC PARAMETER ESTIMATION | 23 |
| Error Analysis of TLRS Tracking LAGEOS | 24 |
| DISCUSSION | 28 |
| REFERENCES | 33 |
| FIGURES | |

# INTRODUCTION

The primary goal of the Laser Geodynamics Satellite Mission is to employ precision laser tracking observations to measure the dynamic behavior of the earth at the centimeter level of accuracy. The currently available precision of the laser observations is better than five centimeters and is progressively improving. LAGEOS is in a more stable and predictable orbit than other retro-reflector-carrying satellites, and the perturbation model for the satellite's motion is improving with each set of new observations. Possible errors in the laser observations themselves will become increasingly important in their application to derive important geodetic parameters such as the relative movement and deformation of the earth's tectonic plates.

Many of the errors encountered in a laser ranging system can be reduced only through the employment of improved instrumentation. They arise primarily in the time interval measurement resolution and precision, the ability to keep real time, and the stability of the system oscillator. If we exclude from consideration satellite-dependent error sources such as the size or depth of the target and the effect of coherent fading of the laser beam due to retro-reflector non-planarity, the most significant remaining source of error is the correction of the ranging measurement for atmospheric refraction.

The range refraction correction is susceptible to errors in our assumptions concerning atmospheric composition and homogeneity, as well as in the numerical approximation to an analytical model. A further source of error in the refraction model arises in the measurements of the meteorological conditions on which the approximations to the atmosphere are based. These quantities are limited by instrumentation accuracy and can never be completely free of operator observation and transcription errors unless they are automatically recorded.

We have considered the refraction effect from three perspectives. An analysis of the axioms on which the currently accepted correction algorithms were based was the first priority. The integrity of the meteorological measurements on which the correction model is based was also considered and a large quantity of laser observations was processed in an effort to detect any serious anomalies in them. The effect of refraction errors on geodetic parameters estimated from laser data using the most recent analysis procedures was the focus of the third element of our studies. The reported results concentrate on refraction errors which we have found to be critical in the eventual use of the data for measurements of crustal dynamics. Details of analyses in which refraction or data error was found to be insignificant are not reported. One of the criteria which we have adopted to determine significance is that a satellite range observation taken at $20^{0}$ elevation or a tower calibration measurement of 10 km. two-way distance be perturbed by more than one centimeter. Several of our experiments merely confirmed the results published by other workers in the field of atmospheric refraction. We have occasionally dwelt upon the details of individual sets of measurements to illustrate points concerning the general conclusions which we discuss in the final section of this report.

## REFRACTIVITY AT OPTICAL FREQUENCIES

The determination of the range between a laser system and the target presumes a correct value of the velocity of propagation of the laser energy as well as the time it takes the laser energy to travel to the target and return. In propagating through the atmosphere, the laser energy is slowed and suffers geometric bending. Both effects can be explicitly determined if the true index of refraction along the path of propagation is known. For ranging systems where accuracy and precision to a few tens of centimeters is required, simple atmospheric models and nominal measurements of atmospheric conditions are sufficient. However, for those systems where range accuracy better than a few centimeters is desired, more complex atmospheric models and better atmospheric parameters are required for accurate correction of the propagation velocity.

The atmospheric refraction correction applied to GSFC laser range data is computed from the formulation developed by Marini and Murray (Ref. 0). The correction is computed as a function of the laser wavelength, the station coordinates, the local temperature, pressure and relative humidity, and the elevation angle of the satellite. Safety requirements restrict the elevation angle at which the lasers acquire observations to be above twenty degrees.

### The Dry Term

The formula adopted by Marini and Murray for the phase refractivity N of dry air is that established in Resolution No. 1 of the 13th General Assembly of the I.A.G. (Ref. 1):

$$N = 10^6 (n-1)$$

$$= \left[287.604 + \frac{1.6288}{\lambda^2} + \frac{0.0136}{\lambda^4}\right] * \frac{P}{T} * \frac{273.15}{1013.25}$$

$$= \left[77.53174 + \frac{.43908}{\lambda^2} + \frac{.00367}{\lambda^4}\right] * \frac{P}{T}$$

in which $n$ is the refractive index of dry air

$\lambda$ is the wavelength of light

$P$ is the atmospheric pressure in mbars

and $T$ is the temperature in $^{o}K$.

The expression is based upon the work of Barrell and Sears (Ref. 2) who investigated the refraction and dispersion of dry, $CO_2$-free air by means of an interference refractometer. They give an accuracy of $\pm 0.01*10^{-6}$ to their formula and quote a term (also adopted in the Marini and Murray treatment) for the effect of humidity.

The group refractivity $N_g$ of air is arrived at through application of the dispersion formula

$$N_g = N - \lambda \frac{dN}{d\lambda}$$

$$= N - \lambda \left[ \frac{-2*.43908}{\lambda^3} - \frac{4*.00367}{\lambda^4} \right]$$

$$= \left[ 77.53174 + \frac{1.31726}{\lambda^2} + \frac{.01833}{\lambda^4} \right] * \frac{P}{T}$$

$$= 80.343 \left[ 0.9650 + \frac{0.0164}{\lambda^2} + \frac{.000228}{\lambda^4} \right] * \frac{P}{T}$$

$$= 80.343 \ f(\lambda) \ \frac{P}{T}$$

$$= 80.343 \ \frac{P}{T} \text{ for red light of } \lambda = .6943\mu$$

and $$= 80.343*1.023 * \frac{P}{T} \text{ for green light of } \lambda = .5322\mu$$

Green light will thus be refracted by an amount 2.3% greater than red light for given atmospheric conditions.

In the comparison by Barrell and Sears of their formula with those given by earlier workers they note good agreement (within .04%) with Perard (Ref. 3) and Kosters and Lampe (Ref. 4). However, their results differ from those of Meggers and Peters (Ref. 5) by 0.21% for red light and 0.27% for green light. Meggers and Peters would thus give a refraction correction approximately 2 cm. shorter than the Marini Murray formulas for a 20° elevation range observation using a green laser for which the total refraction effect is about 7 meters.

The important effect of Meggers and Peters' apparently erroneous dispersion formula on standard spectroscopic tables which had been in use for many years, was pointed out by Edlen (Ref. 6). In a later paper, Edlen (Ref. 7) compared more recent experimental results (up to 1961) with his own dispersion formula for which he claimed an accuracy of 1 part in $10^9$ and which agrees with that due to Barrell and Sears to better than $1.4*10^{-8}$ (.0005%). We must therefore conclude that the expression for group refractivity chosen by Marini and Murray is accurate enough to describe the behavior of light in the visible spectrum to sub-millimeter levels for any practical laser ranging measurement.

## The Wet Term

The effect of water vapor in the atmosphere is given in the Marini Murray formulation as

$$N_g^w = -11.3 \frac{e}{T}$$

in which

$N_g^w$ is the wet term of group refractivity and

e    is the partial pressure of water vapor in mbar which can be obtained from

$$e = \frac{R_h}{100} *6.11*10** \left[\frac{7.5(T-273.15)}{237.3+(T-273.15)}\right]$$

where $R_h$ is the relative humidity.

At a temperature of 300°K, a relative humidity of 100% would yield a partial pressure e = 35 mbar which gives a wet component of refractivity amounting to $1.33*10^{-6}$ (or about 0.5%). This could amount to 1.5 cm in the 3 meter round trip tower calibration correction for a tower located 5 km from the laser site. To restrict the error due to refraction in the wet atmosphere to one centimeter in such a calibration measurement, the relative humidity only needs to be measured very crudely and need only be applied if it is greater than 50%. To limit the error in the dry refractivity term to one centimeter in the tower calibration observation, the average pressure over the tower distance must be known to 4 mbar and the average temperature to 1°C.

REFRACTION CORRECTION OF SATELLITE MEASUREMENTS

The model adopted by Marini and Murray for the correction of an optical path through the vertical atmosphere was based on an exhaustive study of the literature on atmospheric correccion formulae for tracking data. To match the centimeter level accuracy of the laser systems at low elevation angles, the integral evaluations of the group index of refraction along the phase path given by Saastamoinen (Ref. 8) are incorporated into Marini's continued fraction form of the range correction (Ref. 9).

Marini and Murray found that the relative accuracy of the finally chosen refraction model was better than one centimeter when compared to corrections computed from ray-tracing radiosonde profiles. They point out that errors caused by factors common to both methods are not in evidence in their tests. These include the equations for the group refractive index, the errors in which we have found to be small. The common assumption of hydrostatic equilibrium is noted by the authors, and the hydrostatic equation on which they base their atmospheric model is also implicit in the ray-tracing method through its use to infer the heights of the radiosonde observations. We are unable to question this axiom of atmospheric modelling and have in fact relied on the hydrostatic equation in a similar treatment of radiosonde observations which we describe below in an attempt to place a bound on a final source of error in the Marini Murray model: the assumption of horizontal homogeneity.

The refraction correction ΔR in meters to a laser range measurement finally arrived at in the Marini Murray treatment is

$$\Delta R = \frac{f(\lambda)}{f(\phi,H)} \quad \frac{A + B}{\sin E + \dfrac{B/(A+B)}{\sin E + 0.01}}$$

in which

$$A = .002357P + .000141e$$

$$B = (1.084*10^{-8})\,PTK + (4.734*10^{-8})\,\frac{P^2}{T^2} * \frac{2}{(3-1/k)}$$

$$K = 1.163 - 0.00968 \cos 2\phi - 0.00104T + 0.00001435P$$

E is the true elevation of the satellite

$$f(\phi,H) = 1 - .0026 \cos 2\phi - .00031H$$

$\phi$ is the latitude of the laser site

H is the altitude of the laser site in km.

and $f(\lambda)$, P, T, and e are as defined above

The expression can be linearized to the approximation

$$\Delta R \sim .0072P + 0.0004e + .00000025PT$$

for $E = 20^{\circ}$

and P = 1000mbar, T = 300°K and e = 20mbar(50%R.H.)

If the error in the range correction is to be limited to one centimeter the surface pressure must therefore be known to 1.5mbar, the water vapor pressure to within 60 units of percentage relative humidity and the surface temperature to 40°C. These accuracies are clearly within the range of properly calibrated instruments and errors in the refraction correction due to problems with surface measurements will be due to any undetected variation in them over the satellite pass and errors in reading and recording the observations.

## Variations in the Real Atmosphere

The real atmosphere varies both temporally and in three-dimensional space. The time-variation of atmospheric turbulence has been found by Gardner (Ref. 10) to affect satellite range measurements to an insignificant level for most combinations of turbulence strength, scale size and propagation path length. However, for horizontal paths near the earth's surface, such as those used for laser system delay calibration links, centimeter level errors were found due to turbulence.

The effects of an atmosphere which varies in three dimensions have been investigated by Iyer and Bufton (Ref. 11), who show that assymetry in the refractive index could be accounted for by expressing the range correction as a series of terms. An estimate of the higher order correction terms was obtained and can be seen to be in quantitative agreement with the horizontal gradient effect determined by Gardner (Ref. 12). Meteorological data from the Haven Hop network of weather stations located near Washington, D.C. was considered in each of these studies. A correction formula which compensates for the gradient effect was developed by Gardner (Ref. 12) and evaluated by Gardner et al. (Ref. 13) by ray tracing through 3-D refractivity profiles generated using the Project Haven Hop radiosonde measurements.

Gardner et al. conclude that the observed errors in the refractivity observations can be reduced using the gradient correction formula of Ref. 12. They note that, at a $20^{\circ}$ elevation angle the sea level gradient error is approximately 5mm. for a horizontal surface temperature gradient of $1^{\circ}C/100km$. The increase in refractivity caused by the negative temperature gradient from the thermal equator toward the colder climates at the poles was clearly evident in the data and gave rise to the dominant systematic component of the gradient correction formula, in which the most significant effect on a range in meters is given by

$$\frac{.06915 f(\lambda)}{\sin E \tan E} (\sin\alpha \, \overline{x} + \cos\alpha \, \overline{y}) \, \nabla(PTK)$$

in which

$f(\lambda)$, E, P, T and K are as defined above,

$\nabla$ is the gradient operator,

$\overline{x}$ is the east unit vector,

$\overline{y}$ is the north unit vector,

and $\alpha$ is the satellite azimuth angle.

A laser range observation taken at $20^{\circ}$ elevation passes through the atmosphere at 10km. altitude at a distance of 10 cot $20^{\circ}$ = 27 km. from the laser site. If the effects on a range measurement of variations in atmospheric conditions up to 10 km. altitude are to be considered, observations at the spacing of a few tens of kilometers should be studied. In the following section we describe an assessment of the effect on the refraction of laser ranges of horizontal gradients measured at this short spatial interval.

## Analysis of Radiosonde Observations in New Mexico

A series of radiosonde observations was collected during the Prototype Artillery Subsystem (PASS) Project (Ref. 14). One of the purposes of this project was to collect a large volume of atmospheric data to be used for further research and development, particularly in the areas of sound ranging applications and ballistics. Observations of temperature, pressure and relative humidity were collected in November 1974 by radiosonde instruments mounted on balloons launched from several sites in White Sands, New Mexico. The close temporal separation of many of the vertical profile measurements (within one half hour) provided a useful attribute for studies of horizontal gradient effects. The close spatial separation of the launch sites (several dozen kilometers) allows an assessment of shorter wavelength variations than were observable in the Haven Hop Project, in which the stations were separated by several hundred kilometers.

On the other hand, the limited vertical profile extent (up to 300 mbars) placed a restriction on the measured vertical profiles, and the close spacing of the sites limited the grid-size required for detecting the trends at lower spatial frequencies that were provided by the Haven Hop observations.

## Three Dimensional Ray-Tracing Procedure

A three-dimensional ray tracing code was developed to investigate real and theoretical variations in horizontal refractivity. The three dimensional refractive structure of the atmosphere is specified by interpolation among vertical refractivity profiles specified above (up to) nine grid points on the ground. The ray path linking the laser and the satellite is obtained by choosing an approximate initial ray direction and integrating the ray trace equation

$$\frac{d}{ds}\left(n \frac{d\bar{r}}{ds}\right) = \nabla n$$

outwards toward the satellite. Here, n denotes the phase refractive index, s is a distance along the ray path, $\bar{r}$ is a vector designating a point on the ray, and $\nabla$ is the gradient operator. The direction and amount of miss is used to update or correct the initial ray direction and a new path is computed. This procedure is iterated until the ray hits the satellite center with an acceptably small error.

Once the correct ray path has been found, the refraction correction is computed and consists of two terms: the group delay correction

$$\int (n_g - 1) ds$$

and a geometric correction

$$\int ds - R.$$

In these equations, $n_g$ denotes the group refractive index and R is the true satellite range along a straight line path.

Numerical Methods

The refractivity n(h)-1 and its vertical gradient $\partial n/\partial h$ are constructed above each of the grid points on the ground at regular intervals of height. The refractivity is computed using Owens formulae (Ref. 15) from vertical profiles of temperature, pressure and relative humidity. When the refractivity at an arbitrary altitude h and horizontal position (X,Y) is required, it is obtained by interpolation. First, values of n(h) and $\partial n/\partial h$ are obtained by four point Lagrange interpolation on each of the vertical profiles. N(h,X,Y), $\partial n(h,X,Y)/\partial h$, $\partial n/\partial \theta$ and $\partial n/\partial \phi$ (where $\theta$ and $\phi$ are latitude and longitude) are then obtained from a linear two dimensional interpolation using up to six grid points.

The integration of the ray path differential equation is carried out using a modified Hamming predictor-corrector method with variable step size, initiated by an iterated Runge-Kutta scheme. Once the ray path has been found (using a Regula Falsi technique for iteration), the group delay is computed. The path is divided into segments which are short near the ground and increase in length using a twelve point Gaussian quadrature and summed to give the total group delay correction.

The temperature profile assumed for altitudes above the radiosonde data was that given in the U.S. Standard Atmosphere 1976 (Ref. 16) for altitudes at 11, 20, 32, 47, 51, 71 and 84.5 km. This standard profile is shown in Figure 1 and was used to supplement the radiosonde data above 300mbar (about 9 km.) and alternatively to extrapolate upwards a profile based only on surface temperature and assuming a constant lapse rate up to the 11 km. value of the Standard Atmosphere profile.

The surface observation of pressure was then combined with the temperature profile through the hydrostatic equation to produce the corresponding pressure profile.

## Assessment of the Vertical Profile Observations

The radiosonde observations were of limited value for making a full assessment of spatial trends in the atmosphere due to the limited spacing of the launch sites and the drifting of the balloons during ascent. The coordinates of balloons launched within a one half hour interval on November 2nd, 1974 is shown in Figure 2. By the time the balloons had reached 500 mbar (about 7 km.) they had drifted through a distance comparable to the launch site spacing. However it can be seen from Figure 2 that they had maintained approximately the same horizontal separation during ascent, and can therefore be used to monitor horizontal gradients in a consistent space whose upward direction is at a nearly constant angle to the vertical.

In order to simplify the quantitative assessment of the radiosonde observations to which we are limited, the launch sites were placed on a regular rectangular grid (denoted as "ideal position" in Figure 2) with a longitude spacing of 24 km. and a latitude spacing of 16 km. Our model assumed a laser site L placed at the grid point shown, tracking at a number of elevation angles through the profiles above the grid points and at azimuths in the directions N, NW, W, SW and S of L. The ideal positions of the launch sites are always farther from the laser than their real positions, and thus the horizontal gradient levels inferred in the ray-tracing procedure will be conservative.

The real temperature profiles for the experiment of November 2nd are shown in Figure 3, together with those approximated by a constant lapse rate between the surface measurements and the 11 km. value of the Standard Atmosphere profile. A common feature between 4 and 5 km. in each profile indicates the capability of the observations to monitor real variations. The shaded areas of Figure 3 are measures of temperature changes which would not be adequately reflected in the constant lapse rate profiles.

The differences in temperature from the laser profile as a function of altitude for the November 2nd data is shown in Figure 4, which indicates a temperature range of about 5°C at each altitude level. Although the observation error cannot be excluded as a source of these apparent temperature gradients, the overall consistency of the trends suggest that variations of a few degrees are present in the real atmosphere. The precision of radiosonde instrument has been assessed at 1°C at the surface varying linearly to 2.5°C at 30 km. (Ref. 17). Temperature differences of several degrees at the surface and at altitude are shown in Figure 5 for the November 2nd experiment together with two other cases a few days later.

## The Effect of Temperature Gradients on Refractivity

Under the assumptions of vertical ascent and linear extrapolation outside the ideal grid, the ray-tracing procedure predicts the effects on a range measurement at 20° elevation as shown in Figure 6a. Figure 6b indicates the refraction effect if a constant temperature lapse rate from the surface to 11 km. is assumed. The level of the effects is similar for either model of temperature profile but there is little similarity in the patterns predicted by each model.

In Figure 7 the refraction effect on a 20° elevation range observation on November 2nd is shown for the models described above, together with that due to Marini-Murray, which assumes no horizontal gradient between the profiles. The contribution to the refraction effect from each segment of the atmospheric profiles is shown in Figure 7 and plotted in Figure 8 as the difference from the Marini-Murray model value. The effect of temperature gradients on refraction is seen to be greatest at about 10 km. The very large refraction effect at this altitude predicted by the real data balances a contribution of opposite sign at lower altitudes.

The detailed analysis of real temperature observations indicates very high sensitivity of the refraction effect to the temperature gradients inferred by our procedure and is complicated by the drifting of the balloons. The assumption of a constant lapse rate below 11 km. based on surface temperature yields a more stable refractivity effect and corresponds more closely to the assumptions of Marini-Murray and Gardner (Ref. 12) about the behavior of the atmosphere. We therefore adopted this simpler model in a more exhaustive study of the full PASS data set.

All cases in which there were surface observations of temperature and pressure within one half hour from each of the six sites shown in Figure 2 were chosen. The ideal site positions were adopted and the effect on a 20$^{0}$ elevation range from the laser site L was computed for azimuths corresponding to the N, NW, W, SW and S directions. The effect in centimeters is shown in Figure 9 for each of the thirty-three available cases. The table of Figure 9 is divided into four time periods of approximately one week each and the average weekly effect tabulated for each direction in Figure 10. Neither the weekly breakdown of the refraction effect nor the total variation over the approximately monthly time span suggests systematic variation in azimuth over the 24 km by 16 km spacing. The variation can be seen to amount to almost 2 cm. over the full experimental period. The implications of these results are discussed in the last section of this report.

INTEGRITY OF METEOROLOGICAL OBSERVATIONS

During the early months of 1979 four mobile lasers were co-located with the GSFC stationary system (STALAS) in Greenbelt, Maryland. The relative locations of the systems are shown at the top of Figure 11a and they are denoted by the letters A, B, C and D. The heights of the lasers on a reference ellipsoid, determined from the laser observations taken during the co-location tests were STALAS: 15 m., A: 5 m., B: 14 m., C: 14 m. and D: 6 m. The meteorological measurements collected by each system to drive the refraction model were available in the format for the ranging observations and were tabulated for each pass of LAGEOS data during which at least one mobile laser obtained observations simultaneously with STALAS.

The time of day, the value of the temperature, pressure and relative humidity at STALAS and the difference between the simultaneously observing stations' meteorological reading and that of STALAS are tabulated in Figure 11a for three occasions in February 1979. Figures 11b and 11c show similar information for simultaneous LAGEOS pass acquisitions in March and April 1979 respectively. The most striking difference in the readings at each site is in relative humidity which fortunately is the parameter to which the refraction correction is least sensitive. However, errors in the relative humidity as large as 59% (on 3-22 at 10 hrs) would produce errors of almost one centimeer in the refraction correction of a $20^{0}$ elevation range or in that of a calibration measurement at 10 km two-way tower distance. There appears to be no systematic difference in relative humidity, pressure or temperature between the various sites but the difference between the sites A, B and STALAS, which are located within a few dozen meters can be seen to amount to 4°C and 4 mbars on occasion. It must be assumed that this difference is due to errors in the reading of the instruments for such closely spaced observations. An error of 4°C would produce an error of 4 cm in a 10 km two-way tower calibration measurement and would certainly confound any attempt to monitor horizontal temperature gradients to apply a gradient correction term. A pressure error of 4 mbar would cause a refraction error of 0.4% in all satellite ranges taken from a station at sea level. This would amount to a little less than 3 cm for a 20° elevation ranging observation.

In Figures 12a, b and c the differences in temperature and pressure radings taken at the stationary Greenbelt laser (STA) and a mobile laser (MOB) are shown, for a collocation period in early 1980. Although temperature differences as large as 3°C are occasionally recorded, no systematic temperature difference can be seen. On the other hand, the pressure recorded at the mobile site is systematically lower than that at the stationary laser. The average bias of the mobile system during the months of March and April amounts to -3.5 mbar. In a comparison of these measurements with those collected by the stations of the National Weather Service, Gibbs and Mayer (Ref. 18) suggest that the error occurred in the barometer at the mobile site. Large pressure biases were also found at the Haystack, Mass. and Patrick Air Force Base, Florida stations as well as large, random temperature differences with the NWS stations in Goldstone, California.

## GEODETIC PARAMETER ESTIMATION

The approach conventionally adopted for the estimation of geodetic parameters from laser range data is based on a Bayesian weighted least squares orbit determination scheme such as the GEODYN system (Ref. 19). Laser data, preprocessed to include calibration and atmospheric refraction corrections, are reduced to simultaneously estimate the satellite orbit, components of station location at one or more sites, and possibly orbit model characteristics, such as an atmospheric drag or solar radiation pressure scaling factor.

The accuracy of geodetic quantities such as relative station location estimated from laser observations is critically dependent on the design of the experiment. When data from near-earth satellites are used, the analyst's main preoccupation is to design an experiment to reduce the effects of dynamic force model error. The final data configuration has usually been that in which as many observations have been acquired in as short a period of time as possible. More subtle designs will be required to reduce the effect of refraction model error.

A simple test has been made, based on a technique used to measure relative station heights and interstation chord distances between lasers in the West Atlantic tracking GEOS-3 (Ref. 20). Single passes of data of less than ten minutes in length were employed to reduce the effect of the dominant source of error: the geopotential model. The geodetic measurements were made with a precision of approximately 15 cm. if all known error sources are considered and a perfect refraction model is assumed. If we assume the rather large error of 1% in the refractive modulus used in preprocessing the observations, the inter-station baselines increase by up to 8 centimeters. The orbital fits to the range data remained at the observation noise level of 7 cm. even when the refractive modulus was increased by 10%, as the refraction error was completely absorbed by the estimated parameters. Refraction errors will actually arise in a more random pattern than the elevation-dependent bias assumed in this test, which nevertheless suggests that the refraction model must be carefully considered as an error source in geodetic parameter estimation at the centimeter level.

## Error Analysis of TLRS Tracking LAGEOS

The LAGEOS orbit is high enough that it is much less sensitive to drag, solar radiation pressure and geopotential model error than are other laser geodetic satellites in near-earth orbits. The accuracy of currently available dynamic orbit models allows orbital fits to the range data at the noise level of less than 10 cm. for several revolutions and of less than 25 cm. for orbital arc lengths of several days (Ref. 21). At this level of precision the effects of instrumentation and refraction error may approach that in the dynamic model.

To investigate the effect of refraction error in comparison to other sources of error, a LAGEOS tracking configuration in the western United States suggested by

Christodoulidis and Smith (Ref. 22) was considered. It is depicted graphically in Figure 13 and is comprised of two stations considered fixed at San Diego (SANDIE) and at Quincy, California. The relative positions of transportable lasers at T1 and T2 (a north-south baseline) or at T1 and T3 (an east-west baseline) were the parameters whose estimates were investigated using the ORAN error analysis system (Ref. 23) under a variety of circumstances.

For the case in which two transportable lasers were available for simultaneous occupation of the sites, all possible LAGEOS ranging measurements above $20^{\circ}$ elevation angle from the four stations were simulated during a 5 day time period. The noise level of the observations was assumed to be 10 cm. at a repetition rate of 1 second. The error analysis system computes the effects of perturbations to the force and measurement model on the estimated parameters, which in this case were the six elements of the orbit and three position components of each transportable system. For the cases in which 100% efficiency was assumed for the laser systems, the effects on the baseline between the transportable systems caused by errors in the listed unadjusted parameters are shown in Figure 14 in the columns labelled 100%. The two alternative configurations (north-south and east-west) are represented graphically above the corresponding table. The error sources considered were 25 cm. in each component of the location of the fixed stations, 10 cm. biases in the laser range observations, a 1% error in refractivity, an error in the universal constant GM of 1 part in $10^{7}$ and a measure of gravity error in the variance-covariance matrix of the GEM-9 geopotential model (Ref.

24). The total error in the north-south baseline is shown in Figure 14 to be 2.9 cm. and contains a significant effect due to refraction and instrumentation biases. These observation model errors are less important in the east-west baseline error estimate, which amounts to 2.2 cm., largely due to GM error. A more realistic situation in which 50% efficiency is assumed for the laser systems was also simulated and the results shown in Figure 14. In this case only 50% of all available passes were considered in the data reduction scheme. A high sensitivity to geopotential model error is indicated in the baseline error estimates which amount to 11.3 cm. for the north-south configuration and 6.2 cm. east-west. The effects of refraction and instrumentation bias do not significantly increase when the system efficiency is decreased to 50%.

A situation in which we are afforded the luxury of only a single transportable laser ranging system was also considered. In this case the transportable system must occupy the sites between which the baselines must be estimated in separate time periods. In the simulations, consecutive 5-day occupations were assumed and Figure 15 shows the results for 100% and 50% values of system efficiency. The degradation in system efficiency is seen to be far more critical in the case of consecutive transportable laser site occupations than in the case where simultaneous ranging is possible. In particular the effect of 1% refraction error amounts to 3.9 cm. in the east-west baseline error estimate. In order to approach the results possible with 5 days of simultaneous data, the lasers require 30 days of continuous tracking at 50% efficiency in two consecutive site occupations of a single transportable system. The effects of the unmodelled errors on baseline estimates from this extended period of deployment is also shown in Figure 15. The effects of refraction error are reduced to 1.6 cm. in the north-south baseline and 0.7 cm. in the east-west baseline estimate.

DISCUSSION

The Marini-Murray refraction model which is applied to the laser data collected as part of the Crustal Dynamics Program is appropriate within the limitations stated by its authors. Marini and Murray's treatment is based on some simplifying assumptions about the meteorological conditions above the laser site. It was found to produce results in essential agreement with those given by our ray tracing procedure, even when constraints on the variations in vertical profiles of temperature were relaxed. The correction algorithm is simple and the correction is well-defined from easily observed surface measurements.

The main limitation of the current model is in its requirement for spherical symmetry in the atmosphere above the laser site. This restriction is stated by the authors and has been studied by several workers since the original correction algorithm was published. The observations upon which studies of horizontal gradients had been based before our analysis were made at meteorological observing stations whose closest separation was about 100 km. and whose largest separation was about 600 km. (see Ref. 13). This data configuration revealed relatively small average effects on the refraction of laser range observations. The stations were spaced far enough apart to detect the refraction effect due to the temperature gradient between the pole and the equator.

A laser observation of $20^{o}$ elevation passes through the lower tropopause at a horizontal distance of 30 or 40 kilometers from the station. It is at this altitude that any horizontal gradients in the atmosphere would be most critical. We have considered possible gradients as measured by radiosonde balloons separated by distances between 10 km. and 35 km. The benefits of a spacing commensurate with the surface distance travelled by a low elevation ranging signal are however limited by the errors in the extrapolation necessary to infer the atmospheric structure outside our 6-station grid. The short time intervals (less than half an hour) between observations of the vertical profile were compatible with the time span of a satellite pass and would therefore indicate the effects of any gradients such a pass might experience. The limited altitude (300 mbars) of the vertical profile measurements prevented any direct measurement of temperature gradients closer to the tropopause. Our results therefore suffer from possible errors of extrapolation in the vertical direction, which would tend to exaggerate any real variation.

Some stability was restored to the gradient measurements by assuming a model for conditions aloft similar to that on which the Marini-Murray model was based: a constant temperature lapse rate based on surface observations. Errors in horizontal extrapolation still remain with this approach and will exaggerate gradients measured in a small grid, in which there is little redundancy of information to eliminate effects with very short spacial wavelength or those due to instrumental error. The simplification of the vertical atmospheric structure also eliminates the effect of balloon drift which made the detection of any systematic trends in the gradients difficult from the real vertical profile observations. A range measurement at 20° elevation passing through an atmosphere with the computed horizontal gradients would differ by several centimeters from that in a spherically stratified atmosphere.

The analysis of the real observations was finally reduced to the consideration of qualitative evidence of temperature gradients at altitude. Systematic patterns of temperature variations were detected in vertical profiles which were evenly spaced in the vertical and relative horizontal directions, as they were measured from balloons with nearly consistent drift rates. These temperature variations (up to 5°C at surface and at altitude) are too large to be included in the accepted error budget for the instruments. Their systematic nature supports our contention that real gradients may exist and are not artifacts of measurement error. The inference we draw that horizontal gradients may contribute to several centimeters of error in a pass of low elevation ranging observations is not incompatible with the results of others who have averaged over larger space and time intervals and found smaller effects. We feel however that we have erred in the direction of exaggeration and that these results be considered upper bounds on the effects of refractivity variation.

Assessments of the integrity of the surface observations which are collected at a laser station for inclusion in the refraction correction were not reassuring. Variations of several degrees in temperature were found between observations made at collocated laser sites for which identical meteorological conditions would be expected. This variation could be the result of operator error in reading and recording the instruments or occasional instrument malfunction. It could also be caused by natural variation of temperature over a distance of a few hundred meters. Holdahl (Ref. 25) has observed temperature variations of several degrees centigrade due to stratification in the boundary layer close to the ground. Temperature error in the currently adopted refraction correction procedure will mostly affect tower calibration measurements which are made by the currently deployed laser systems to allow for cable delays which would bias the satellite measurements. Internal calibration procedures would eliminate this possible error source, which could however be reduced if more temperature observations were made in the vicinity of the laser stations and particularly in the direction of the calibration tower. Regular calibration of each station's barometer would reduce the possibility of pressure errors, which dominate the refraction error budget for satellite range corrections.

The precision of the pressure and temperature readings reported with the laser ranging observations slightly complicated our attempt to confirm that the Marini-Murray model had in fact been applied to the ranges. The reported values are truncated to the nearest millibar and degree, although the refraction correction is computed using more precise observations. However, in light of the physical and possibly instrumental limitations on the meteorological values and their application, we do not consider this a serious source of error. Of all the perturbations to the refraction model which we have investigated, this is the simplest to eliminate.

The evidence of variability in meteorological conditions which we have found is not completely unexpected. Variations in pressure and temperature are extremely difficult to predict or model. We feel that the elimination of consequent errors in the refraction model is more effectively accomplished by designing geodetic parameter estimation procedures which include redundancy. The simplest way to introduce this element is to extend the period over which satellite observations are collected to yield a single geodetic measurement. Simulation studies based on a typical experiment have indicated that large refraction errors can be considerably reduced by extending the campaign duration from 5 days to 30 days. This time period is currently required to also eliminate errors in geodetic measurements caused by lack of knowledge of the satellite perturbation model and the relative location of supporting stations. These other elements of the error budget will improve with time due to expected improvements in instrumentation and in the development of a better satellite force model. Improvements in the atmospheric model are unlikely to keep pace with progress in other areas of satellite laser analysis and we must therefore be careful to maintain the integrity of the meteorological observations on which our refraction model depends.

## REFERENCES


0. Marini, J.W. and Murray, Jr., C.W., "Correction of Laser Range Tracking Data for Atmospheric Refraction at Elevations Above 10 Degrees," **NASA X-591-73-351**, Nov. 1973.

1. International Association of Geodesy, Resolution No. 1 of the 13th General Assembly, **Bulletin Geodesique**, 70, p. 360, 1963.

2. Barrell, H. and Sears, J., "The Refraction and Dispersion of Air for the Visible Spectrum," **Trans. Roy. Soc. London**, A238, February 1939.

3. Perard, A., "Dilatometre Fizeau," **Trav. Bur. int. Poids Mes. 19**, 78, 1934.

4. Kosters, W. and Lampe, P., **Physik. Z. 35**, 223, 934.

5. Meggers, W.F. and Peters, C.G., **Natl. Bur. Standards U.S. Sci. Papers 14**, 724, 1918.

6. Edlen, B., "The Dispersion of Standard Air," **Journ. Opt. Soc. America**, 43, 5, May 1953.

7. Edlen, B., "The Refractive Index of Air," **Metrologia**, 2, 2, 1966.

8. Saastanoinen, J., "Contributions to the Theory of Atmospheric Refraction," **Bulletin Geodesique 105-107**, pp. 279-298, 383-397, 13-34, 1972.

9. Marini, J., "Correction of Satellite Tracking Data for an Arbitrary Tropospheric Profile," **Radio Sci.**, 7(2), 223-231, 1972.

10. Gardner, C.S., "Effects of Random Path Fluctuations on the Accuracy of Laser Ranging Data," **Applied Optics**, 15, 253 9-2545, October 1976.

11. Iyer, R.S. and Bufton, J.L., "Corrections for Atmospheric Refractivity in Satellite Laser Ranging," **Applied Optics**, 16, 1997-2003, July 1977.

12. Gardner, C.S., "Correction of Laser Tracking Data for the Effects of Horizontal Refractivity Gradients," **Applied Optics**, 16, 2427-2432, September 1977.

13. Gardner, C.S., Rowlett, J.R., and Hendrickson, B.E., "Ray Tracing Evaluation of a Technique for Correcting the Refraction Errors in Satellite Tracking Data," **Applied Optics**, 17, 3143-3145, October 1978.

14. D'Arcy, E.M., "PASS 500 mb Radiosonde Data," Vols. I and II, **ECOM-DR-77-4**, June 1977.

15. Owens, J.C., "Optical Refractive Index of Air: Dependence on Pressure, Temperature and Composition," **Applied Optics**, 6, 1, 51-59, January 1967.

16. "U.S. Standard Atmosphere, 1976," **NOAA-S/T76-1562**, October 1976.

17. "Meteorological Data Error Estimates," **Met. Group Range Commanders Council Doc. 110-77**, Jan. 1977.

18. Gibbs, B.P. and Majer, V., "Accuracy Assessment of the Atmospheric Correction Used in the NASA Laser Ranging Program," **BTS-FR-81-166**, Sept. 1981.

19. Putney, B., "General Theory for Dynamic Satellite Geodesy," Section 5.4.1, National Geodetic Satellite Program Part 1, **NASA SP-365**.

20. Dunn, P.J., Torrence, M., Smith, D.E. and Kolenkiewicz, R., "Base Line Estimation Using Single Passes of Laser Data," **JGR Vol. 84**, No. B8, July 1979.

21. Smith, D.E., Kolenkiewicz, R., Dunn, P.J. and Torrence, M., "Determinaton of Polar Motion and Earth Rotation from Laser Tracking of Satellites," **Proc. Symp. No. 82**, "Time and the Earth's Rotation," Reidel, 1979.

22. Christodoulidis, D.C. and Smith, D.E., "Prospects for TLRS Baseline Accuracies in the Western U.S.A. Using LAGEOS," **NASA TM 82133**, April 1981.

23. Martin, C.F. and Roy, N.A., "Error Model for the SAO 1969 Standard Earth," "The Use of Artificial

Satellites for Geodesy," **AGU Geophysical Monograph 15**, 1972.

24. Lerch, F.J., Klosko, S.M., Laubscher, R.E. and Wagner, C.A., "Gravity Model Improvement Using GEOS-3 (GEM 9 and 10)," **JGR, Vol. 84**, No. B8, July 1979.

25. Holdahl, S.R., "A Model of Temperature Stratification for Correction of Leveling Refraction," **Bulletin Geodesique 55**, pp. 231-249, 1981.

FIGURE 1. TEMPERATURE PROFILE ASSUMPTIONS
(1976 STANDARD ATMOSPHERE ABOVE 11 KM.)

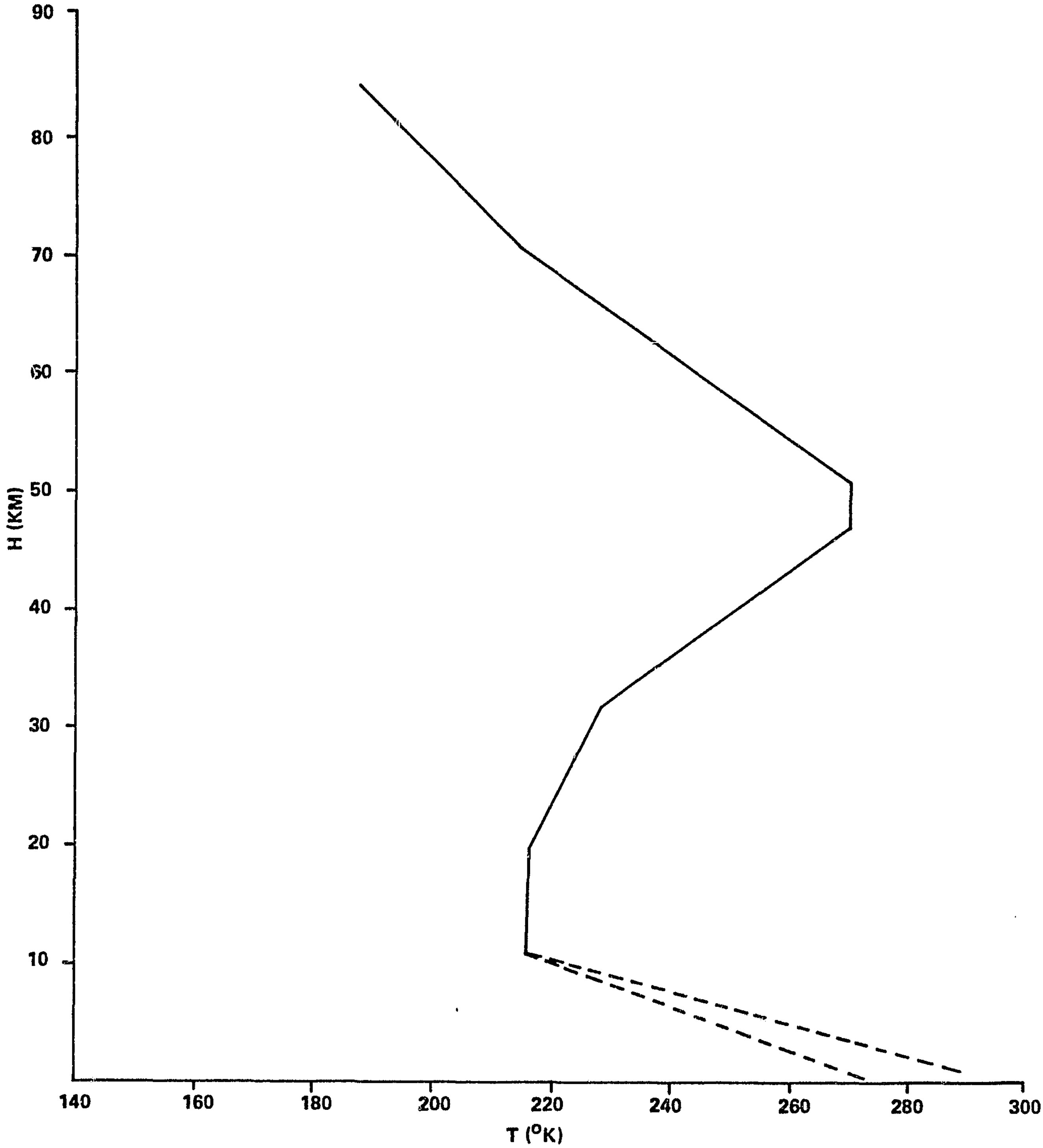

FIGURE 2. BALLOON COORDINATES AT 880 MBAR AND 500 MBAR (11–2–10.30)
(SHOWS DRIFT TO NORTH–EAST)

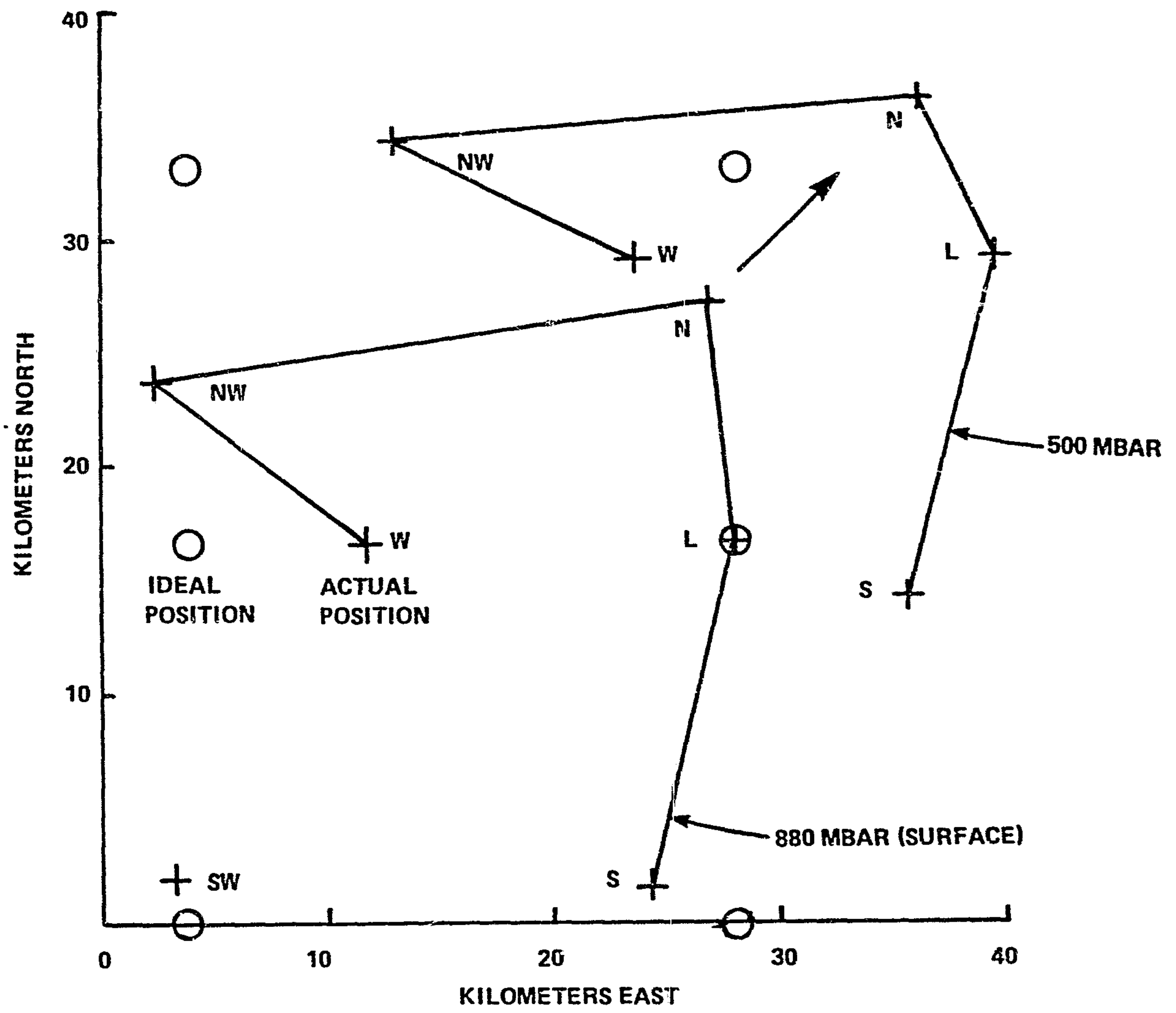

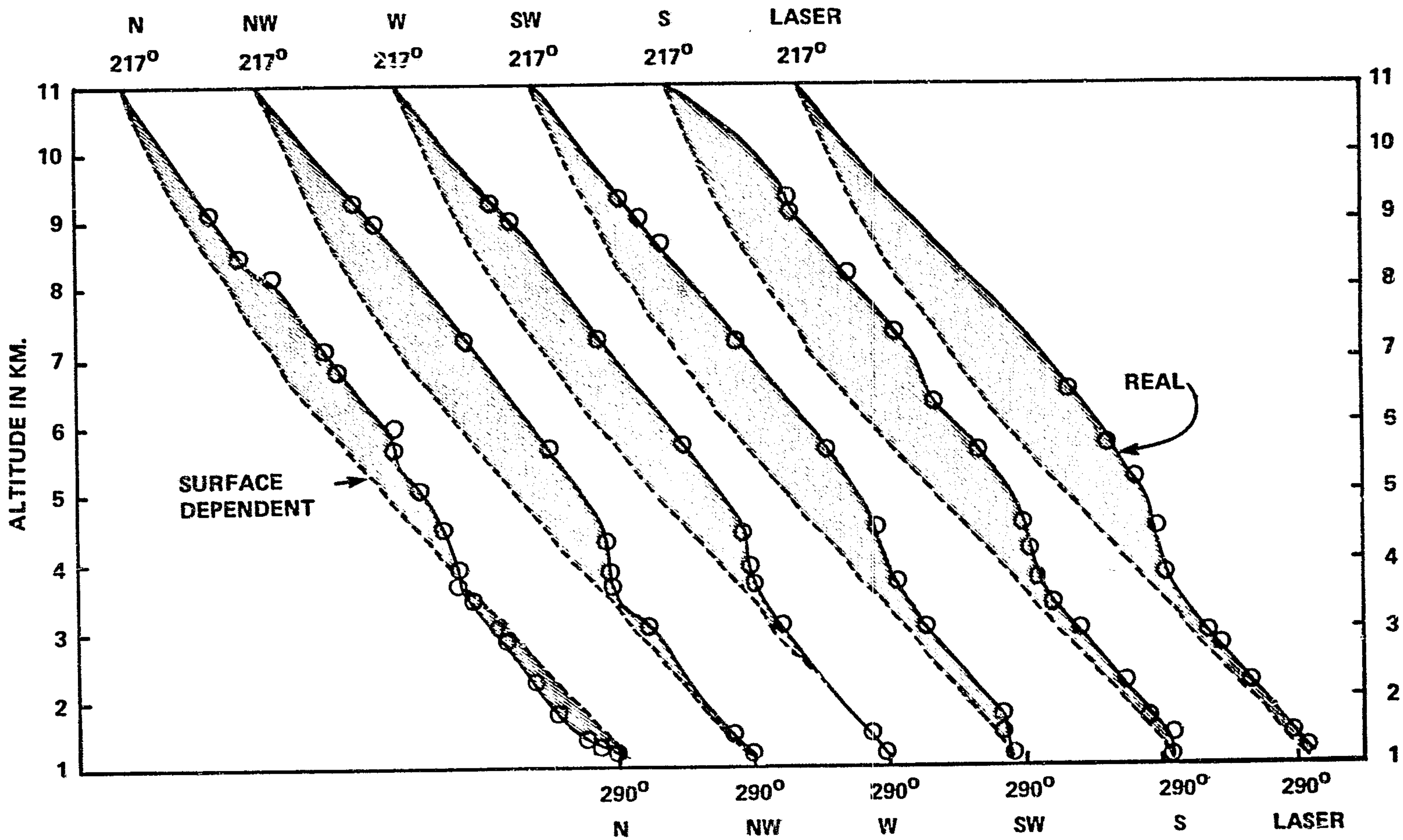


FIGURE 3. REAL TEMPERATURE PROFILES AND PROFILES FROM SURFACE DATA
(THE DIFFERENCE IS SHADED)

| HEIGHT (km) | DIRECTION OF TEMPERATURE DIFFERENCE IN DEG. C | | | | |
|---|---|---|---|---|---|
| | N | NW | W | SW | S |
| 10 | –0.5 | –0.2 | –0.4 | –0.2 | 6.8 |
| 9 | –4.2 | –1.0 | –1.0 | –0.8 | 2.4 |
| 8 | –4.2 | –3.4 | –3.1 | –3.5 | 1.3 |
| 7 | –5.8 | –4.1 | –4.5 | –3.7 | 0.5 |
| 6 | –3.5 | –3.6 | –3.2 | –2.7 | –0.8 |
| 5 | –5.0 | –2.5 | –2.0 | –1.8 | 0.5 |
| 4 | –4.3 | –1.0 | –1.7 | –0.5 | –0.9 |
| 3 | –5.5 | –2.7 | –2.5 | –1.5 | –0.6 |
| 2 | –5.6 | –0.5 | –2.7 | 1.0 | 1.0 |
| 1 | 0.2 | –2.3 | –0.6 | –3.3 | –1.1 |

FIGURE 4. TEMPERATURE DIFFERENCE FROM BASE PROFILE, BY ALTITUDE (ON 11–2–10.30)

| DATE | HEIGHT | N | NW | W | SW | S |
|---|---|---|---|---|---|---|
| | | DIRECTION OF TEMPERATURE DIFFERENCE IN DEG. C | | | | |
| 11–2–10.30 | 10 km | –0.5 | –0.2 | –0.4 | –0.2 | 6.8 |
| | 1 km | 0.2 | –2.3 | –0.6 | –3.3 | –1.1 |
| 11–4–10.30 | 10 km | –1.4 | –3.4 | –2.7 | –3.3 | 2.1 |
| | 1 km | –1.5 | –0.6 | –3.8 | –2.9 | –4.2 |
| 11–6–5.00 | 10 km | –1.5 | 0.3 | –2.4 | –2.9 | 1.3 |
| | 1 km | –4.3 | –3.1 | –3.5 | –3.1 | –2.8 |

FIGURE 5. TEMPERATURE DIFFERENCES AT SURFACE AND AT ALTITUDE

| | DIRECTION OF REFRACTION EFFECT IN CM. | | | | |
|---|---|---|---|---|---|
| DATE | N | NW | W | SW | S |
| 11-2 – 10.30 | –4.1 | –1.0 | –3.2 | –0.3 | 0.6 |
| 11-4 – 8.30 | 1.0 | –1.0 | –3.2 | –0.9 | –2.8 |
| 11-6 – 5.00 | 0.6 | –2.4 | –1.0 | 1.0 | 0.0 |

FIGURE 6a. EFFECT ON 20° ELEVATION RANGE DUE TO GRADIENTS FROM RADIOSONDE DATA

| | DIRECTION OF REFRACTION EFFECT IN CM. | | | | |
|---|---|---|---|---|---|
| DATE | N | NW | W | SW | S |
| 11-2 – 10.30 | –0.2 | –1.7 | –0.7 | –2.8 | –0.8 |
| 11-4 – 8.30 | –1.4 | 1.2 | –3.0 | –0.9 | –4.2 |
| 11-6 – 5.00 | –4.3 | –0.9 | –2.6 | –1.6 | –2.7 |

FIGURE 6b. EFFECT ON 20° ELEVATION RANGE DUE TO GRADIENTS COMPUTED FROM SURFACE DATA

| SEGMENT | REFRACTION EFFECT M–M (cm) | REFRACTION EFFECT S.P. (cm) | REFRACTION EFFECT REAL P. (cm) | RELATIVE EFFECT S.P. (cm) | RELATIVE EFFECT REAL P. (cm) | HEIGHT (cm) |
|---|---|---|---|---|---|---|
| 10 | 5.1 | 5.1 | 5.0 | 0.0 | –0.1 | |
| | | | | | | 29.2 |
| 9 | 14.5 | 14.4 | 14.3 | –0.1 | –0.2 | |
| | | | | | | 21.9 |
| 8 | 30.8 | 30.7 | 30.8 | –0.1 | 0.0 | |
| | | | | | | 16.3 |
| 7 | 53.2 | 53.0 | 55.0 | –0.2 | 1.8 | |
| | | | | | | 12.0 |
| 6 | 73.8 | 73.7 | 76.3 | –0.1 | 2.5 | |
| | | | | | | 8.7 |
| 5 | 84.2 | 84.1 | 83.2 | –0.1 | –1.0 | |
| | | | | | | 6.2 |
| 4 | 84.0 | 84.0 | 81.4 | 0.0 | –2.6 | |
| | | | | | | 4.2 |
| 3 | 77.1 | 77.2 | 74.9 | –0.1 | –2.2 | |
| | | | | | | 2.7 |
| 2 | 67.3 | 67.3 | 66.4 | 0.0 | –0.9 | |
| | | | | | | 1.6 |
| 1 | 56.7 | 56.7 | 56.4 | 0.0 | –0.3 | |
| | | | | | | .7 |

FIGURE 7. REFRACTION EFFECT BY ALTITUDE REGIME ON 20° ELEVATION RANGE DUE TO THREE ALTERNATIVE MODELS:
MARINI–MURRAY (M–M)
SURFACE DATA PROFILES (S.P.)
REAL DATA PROFILES (REAL P.)
WEST DIRECTION ON 11–2–10.30

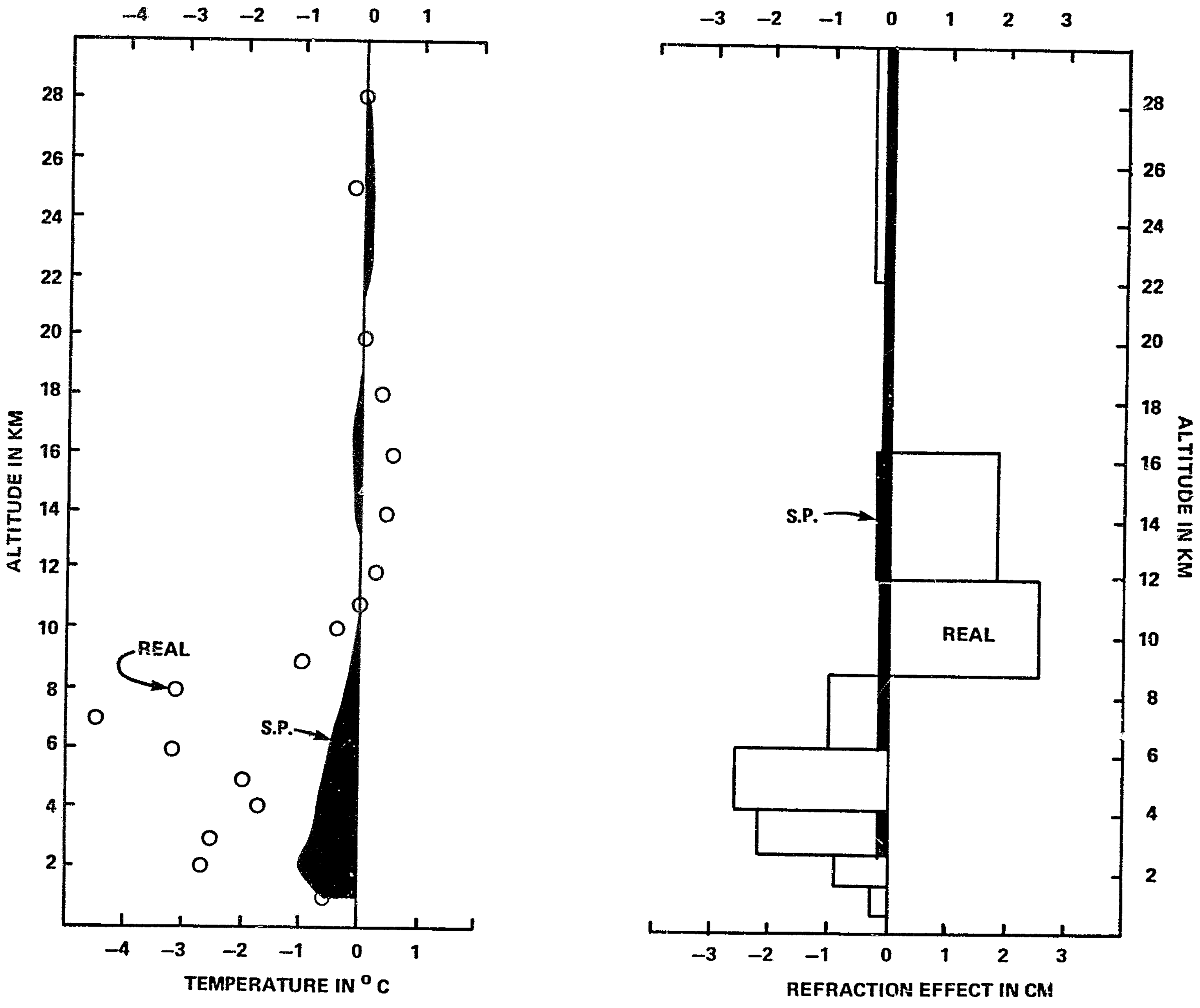


FIGURE 8. TEMPERATURE DIFFERENCE AND REFRACTION EFFECT ON 20° ELEVATION RANGE BY ALTITUDE REGIME (WEST DIRECTION ON 11–2–10.30)

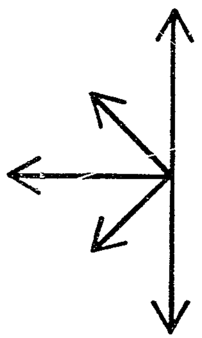

| DAY / HOUR | 1 / 4 | 2 / 8 | 2 / 10 | 4 / 8 | 6 / 5 | 6 / 7 | 6 / 9 | 7 / 4 | 7 / 8 | 7 / 10 | 7 / 12 | 8 / 15 | 11 / 7 | 11 / 9 | 12 / 4 | 12 / 8 | DAY / HOUR |
|---|---|---|---|---|---|---|---|---|---|---|---|---|---|---|---|---|---|
| N | −1 | −1 | 0 | −1 | −4 | −2 | −2 | −3 | −2 | −1 | −4 | −1 | 1 | 0 | −8 | −3 | N |
| NW | 0 | −2 | −2 | 2 | 0 | −1 | −1 | 3 | 0 | −1 | 0 | 0 | 0 | 1 | 1 | 1 | NW |
| W | −2 | −3 | −1 | −3 | −3 | −1 | 0 | 0 | −2 | −1 | −3 | −1 | 0 | 0 | −5 | −3 | W |
| SW | −3 | 0 | −3 | 0 | −1 | −2 | −1 | 0 | −1 | −1 | 0 | −1 | −1 | −2 | −3 | −3 | SW |
| S | (9) | −4 | −1 | −4 | −3 | −3 | −3 | 1 | 0 | −1 | 4 | −1 | 2 | −5 | −3 | −2 | S |

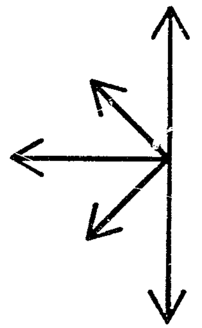

| | | | | | | | | | | | | | | | | | | |
|---|---|---|---|---|---|---|---|---|---|---|---|---|---|---|---|---|---|---|
| N | −6 | −5 | −2 | −2 | −5 | −1 | −3 | 1 | −2 | −2 | 0 | 1 | −1 | −2 | −1 | 0 | −1 | N |
| NW | 2 | 2 | −1 | −2 | 2 | 0 | 1 | −1 | −1 | 0 | 1 | −1 | 0 | 1 | 0 | −1 | 0 | NW |
| W | −2 | −1 | −2 | −2 | −4 | −2 | −1 | −1 | 0 | 1 | 0 | 1 | −1 | −2 | −1 | 0 | 0 | W |
| SW | 1 | −2 | −2 | −2 | 0 | 3 | −1 | 1 | −1 | 1 | 2 | 1 | 0 | 0 | 1 | 0 | 0 | SW |
| S | −1 | 0 | −4 | −3 | −3 | −1 | 0 | −6 | 0 | 0 | −1 | 1 | −1 | −4 | −2 | 0 | −2 | S |
| HOUR / DAY | 4 / 14 | 6 / 14 | 10 / 14 | 12 / 14 | 6 / 15 | 12 / 15 | 4 / 18 | 7 / 19 | 14 / 20 | 16 / 20 | 8 / 23 | 14 / 23 | 13 / 27 | 5 / 32 | 9 / 32 | 11 / 35 | 15 / 35 | HOUR / DAY |

FIGURE 9. HORIZONTAL GRADIENT EFFECT IN CENTIMETERS AT 20° ELEVATION
INDIVIDUAL BALLOON FLIGHTS

| DAYS: | 1–6 | 7–12 | 14–20 | 23–35 | 1–35 |
|---|---|---|---|---|---|
| NO. OF OBS: | 7 | 9 | 10 | 7 | 33 |
| N | –1.6 cm. | –2.3 cm. | –2.7 cm. | –0.6 cm. | –1.9 cm. |
| NW | –0.6 | 0.6 | 0.2 | 0.0 | 0.1 |
| W | –1.9 | –1.7 | –1.4 | –0.4 | –1.4 |
| SW | –1.4 | –1.3 | –0.2 | 0.6 | –0.6 |
| S | –3.0 | –0.6 | –1.8 | –1.3 | –1.6 |

FIGURE 10. AVERAGE REFRACTION EFFECT ON 20° ELEVATION RANGE BY WEEK AND BY MONTH


| LOCAL TIME | | | TEMP IN °C. | | | | | (PR.–1000) MBAR | | | | | R.H. IN % | | | | |
|---|---|---|---|---|---|---|---|---|---|---|---|---|---|---|---|---|---|
| MTH | DAY | HR | S | A | B | C | D | S | A | B | C | D | S | A | B | C | D |
| 2 | 1 | 10 | –4 | | | | 3 | –3 | | | | –1 | 45 | | | | 8 |
| 2 | 2 | 9 | –5 | | | –1 | 0 | 8 | | | 1 | –1 | 44 | | | 1 | –1 |
| 2 | 5 | 9 | –6 | | 5 | | | 16 | | –6 | | | 32 | | –8 | | |

DIFF. FROM STALAS (A–D columns of each group)

VALUE AT STALAS (S column of each group)

FIGURE 11a. METEOROLOGICAL OBSERVATIONS DURING 1979 COLLOCATION (FEB)

| LOCAL TIME | | | TEMP IN °C. | | | | | (PR.–1000) MBAR | | | | | R.H. IN % | | | | |
|---|---|---|---|---|---|---|---|---|---|---|---|---|---|---|---|---|---|
| MTH | DAY | HR | S | A | B | C | D | S | A | B | C | D | S | A | B | C | D |
| 3 | 13 | 9 | –3 | | 1 | | | 19 | | 3 | | | 30 | | 0 | | |
| 3 | 20 | 6 | –1 | 1 | | | | 13 | 0 | | | | 30 | 20 | | | |
| 3 | 20 | 9 | 1 | 0 | | | | 14 | –1 | | | | 70 | –40 | | | |
| 3 | 21 | 9 | 7 | 0 | | | | 10 | 0 | | | | 58 | – 8 | | | |
| 3 | 22 | 6 | 4 | 0 | 0 | | –4 | 16 | –2 | 1 | | 1 | 75 | 2 | –2 | | –45 |
| 3 | 22 | 10 | 0 | 0 | 0 | | | 15 | 0 | 1 | | | 89 | –59 | –1 | | |
| 3 | 23 | 6 | 8 | 0 | –1 | | | 14 | 0 | 0 | | | 66 | 6 | –2 | | |
| 3 | 23 | 9 | 4 | –1 | –1 | | –4 | 12 | –2 | 0 | | 1 | 78 | 5 | –10 | | –48 |
| 3 | 28 | 6 | –1 | | 1 | | –2 | 27 | | –4 | | –4 | 30 | | 0 | | 0 |
| 3 | 28 | 9 | –1 | –3 | –2 | | –5 | 25 | –1 | –1 | | 0 | 30 | 0 | 0 | | 0 |

DIFF. FROM STALAS (TEMP A–D) DIFF. (MBAR A–D) DIFF. (R.H. A–D)

FIGURE 11b. METEOROLOGICAL OBSERVATIONS DURING 1979 COLLOCATION (MARCH)

| LOCAL TIME | | | TEMP IN °C. | | | | | (PR.–1000) MBAR | | | | | R.H. IN % | | | | |
|---|---|---|---|---|---|---|---|---|---|---|---|---|---|---|---|---|---|
| MTH | DAY | HR | S | A | B | C | D | S | A | B | C | D | S | A | B | C | D |
| 4 | 11 | 9 | –1 | 1 | | | | 16 | 0 | | | | 88 | 0 | | | |
| 4 | 18 | 6 | 8 | | | –4 | | 13 | | | 1 | | 78 | | | 2 | |
| 4 | 18 | 9 | 6 | 1 | | –2 | | 13 | 1 | | 1 | | 70 | –12 | | 10 | |
| 4 | 18 | 15 | 12 | | | 3 | | 14 | | | 2 | | 48 | | | –13 | |
| 4 | 19 | 3 | 11 | | | 2 | | 13 | 2 | | | | 74 | | | –34 | |
| 4 | 19 | 7 | 8 | | 1 | –4 | | 15 | | 1 | 1 | | 53 | | –16 | 7 | |
| 4 | 20 | 5 | 9 | | –1 | 0 | | 16 | | 0 | 1 | | 73 | | –23 | –34 | |
| 4 | 20 | 9 | 1 | | 0 | | | 18 | | 0 | | | 35 | | – 5 | | |
| 4 | 21 | 3 | 6 | | 1 | –4 | | 16 | | 2 | 5 | | 77 | | –19 | 13 | |
| 4 | 21 | 9 | 4 | | –4 | | | 16 | | 2 | | | 66 | | 6 | | |

Temperature columns A–D: DIFF. FROM STALAS. Pressure columns A–D: DIFF. R.H. columns A–D: DIFF.

FIGURE 11c. METEOROLOGICAL OBSERVATIONS DURING 1979 COLLOCATION (APRIL)

| LOCAL TIME | | | TEMP IN °C | | (PR.–1000) MBAR | |
|---|---|---|---|---|---|---|
| MTH | DAY | HR | STA | MOB–STA | STA | MOB–STA |
| 2 | 19 | 9 | 9 | –1 | 17 | – 6 |
| 2 | 20 | 10 | 14 | 1 | 10 | –10 |
| 2 | 21 | 7 | 14 | 2 | 7 | – 3 |
| 2 | 21 | 11 | 15 | 0 | 7 | – 1 |

FIGURE 12a. METEOROLOGICAL CONDITIONS DURING 1980 COLLOCATION (FEB)

ORIGINAL PAGE IS
OF POOR QUALITY

| LOCAL TIME | | | TEMP IN °C | | (PR.—1000) MBAR | |
|---|---|---|---|---|---|---|
| MTH | DAY | HR | STA | MOB—STA | STA | MOB—STA |
| 3 | 6 | 12 | 6 | −1 | 17 | −2 |
| 3 | 6 | 17 | 3 | −1 | 18 | −4 |
| 3 | 8 | 13 | 20 | 1 | −7 | −2 |
| 3 | 9 | 12 | 11 | 0 | 5 | −3 |
| 3 | 9 | 14 | 9 | 0 | 6 | −3 |
| 3 | 9 | 17 | 4 | −3 | 6 | −2 |
| 3 | 11 | 14 | 3 | 1 | 1 | −2 |
| 3 | 11 | 18 | 0 | 3 | 9 | −3 |
| 3 | 14 | 13 | 5 | −1 | 8 | −2 |
| 3 | 15 | 16 | 5 | 1 | 21 | −3 |
| 3 | 15 | 20 | 0 | −1 | 23 | −3 |
| 3 | 16 | 15 | 9 | −2 | 20 | −2 |
| 3 | 18 | 14 | 5 | 2 | 16 | −5 |
| 3 | 18 | 15 | 4 | 3 | 18 | −4 |
| 3 | 18 | 19 | 4 | 1 | 20 | −4 |
| 3 | 23 | 13 | 10 | 0 | 11 | −6 |
| 3 | 23 | 16 | 9 | −2 | 12 | −3 |
| 3 | 23 | 19 | 4 | −2 | 12 | −4 |
| 3 | 23 | 19 | 4 | −2 | 12 | −4 |

FIGURE 12b. METEOROLOGICAL CONDITIONS DURING 1980 COLLOCATION (MARCH)

| LOCAL TIME | | | TEMP IN °C | | (PR.–1000) MBAR | |
|---|---|---|---|---|---|---|
| MTH | DAY | HR | STA | MOB–STA | STA | MOB–STA |
| 4 | 1 | 14 | 10 | 1 | 13 | –3 |
| 4 | 1 | 17 | 5 | –1 | 13 | –3 |
| 4 | 1 | 18 | 5 | –3 | 13 | –3 |
| 4 | 18 | 15 | 13 | –1 | 10 | –7 |
| 4 | 19 | 14 | 21 | –3 | 11 | –5 |
| 4 | 19 | 18 | 12 | 0 | 14 | 0 |
| 4 | 20 | 14 | 19 | 0 | 3 | –7 |
| 4 | 21 | 15 | 16 | 0 | 3 | –3 |

FIGURE 12c. METEOROLOGICAL CONDITIONS DURING 1980 COLLOCATION (APRIL)

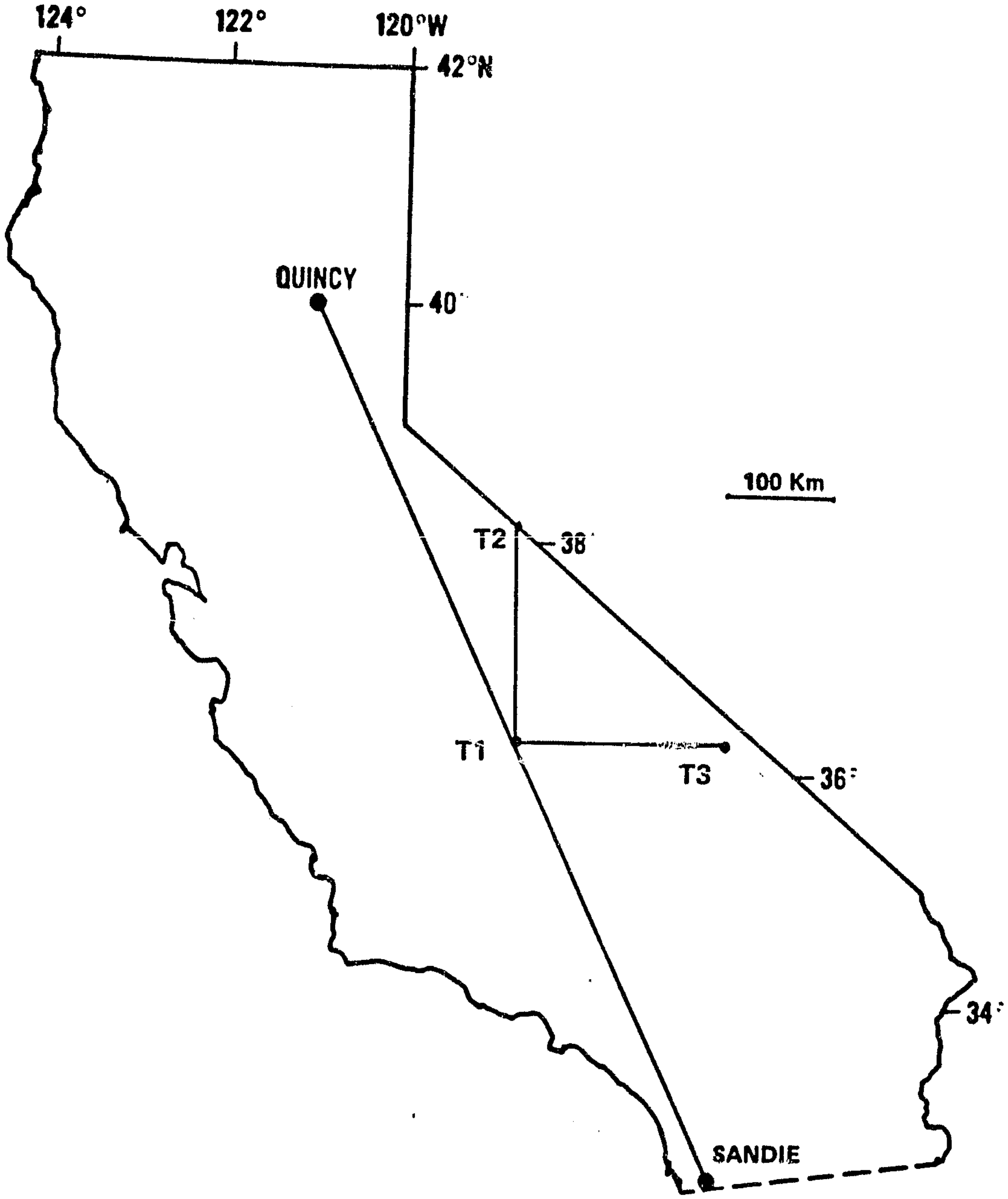


FIGURE 13. TLRS BASELINE EXPERIMENT CONFIGURATION

SIMULTANEOUS

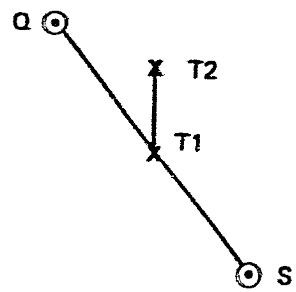


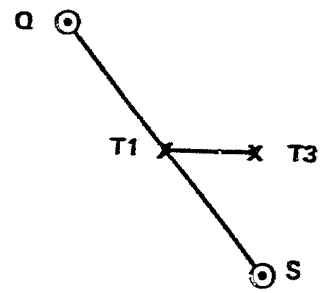


| ERROR SOURCES | NORTH – SOUTH 5 DAYS 100% | NORTH – SOUTH 5 DAYS 50% | EAST – WEST 5 DAYS 100% | EAST – WEST 5 DAYS 50% |
|---|---|---|---|---|
| STATION POSITIONS (25 cm. SANDIE/QUINCY) | 0.1 | 0.6 | 0.2 | 0.3 |
| BIASES (10 cm.) | 1.9 | 1.9 | 0.3 | 0.9 |
| REFRACTION (1%) | 1.5 | 1.5 | 0.1 | 0.6 |
| GM (1 part in $10^7$) | 1.5 | 1.5 | 2.1 | 5.0 |
| GRAVITY (GEM-9 V/C to 10 x 10) | 0.3 | 10.9 | 0.7 | 3.6 |
| NOISE (10 cm. at 1 sec.) | 0.1 | 0.2 | 0.1 | 0.1 |
| TOTAL (RSS) | 2.9 | 11.3 | 2.2 | 6.2 |

FIGURE 14. BASELINE ACCURACIES IN CENTIMETERS FOR TWO TLRS'S: SIMULTANEOUS SITE OCCUPATIONS

CONSECUTIVE

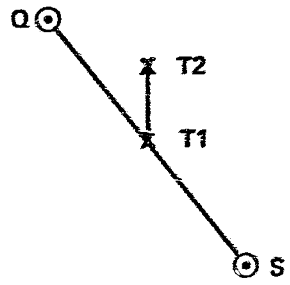


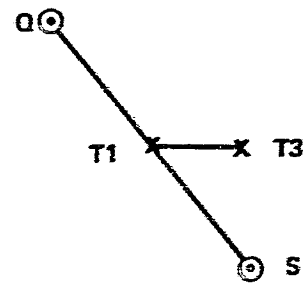


| ERROR SOURCES | NORTH — SOUTH | | | EAST — WEST | | |
|---|---|---|---|---|---|---|
| | 5 + 5 100% | 5 + 5 50% | 30 + 30 50% | 5 + 5 100% | 5 + 5 50% | 30 + 30 50% |
| STATION POSITIONS (25 cm. SANDIE/QUINCY) | 0.2 | 9.6 | 1.3 | 0.7 | 12.9 | 3.3 |
| BIASES (10 cm.) | 2.1 | 3.9 | 2.0 | 0.7 | 8.0 | 1.8 |
| REFRACTION (1%) | 1.7 | 2.2 | [illegible] | 0.5 | 3.9 | 0.7 |
| GM (1 part in $10^7$) | 1.7 | 3.5 | 1.4 | 2.4 | 18.7 | 5.0 |
| GRAVITY (GEM-9 V/C to 10 x 10) | 1.3 | 14.1 | 5.3 | 1.2 | 13.3 | 3.7 |
| NOISE (10 cm. at 1 sec.) | 0.1 | 0.2 | 0.1 | 0.1 | 0.2 | 0.1 |
| TOTAL (RSS) | 3.5 | 18.0 | 6.2 | 2.9 | 27.9 | 7.3 |

FIGURE 15. BASELINE ACCURACIES IN CENTIMETERS FOR ONE TLRS: CONSECUTIVE SITE OCCUPATIONS